

Inelastic behavior and numerical analysis in twin-roll casting process of AZ31 alloy

D. Y. JU^{1,2)}, X. D. HU¹⁾, H. Y. ZHAO²⁾

¹⁾*Saitama Institute of Technology
Fukaya, Saitama, Japan
email: dyju@sit.ac.jp*

²⁾*University of Science and Technology Liaoning
Ashan, Liaoning, China*

IN THIS PAPER, Anand's model, a unified visco-plasticity constitutive model, was employed to simulate the highly nonlinear behavior in the twin-roll casting process. Anand model's parameters were regressed based on compression tests at various temperatures and strain rates for magnesium alloy AZ31. To calculate the thermal mechanical stresses, the thermal flow of twin-roll casting process was simulated firstly; then the stresses were calculated by the imposed thermal flow as the body load, and a small displacement load along roller's tangential direction was imposed simultaneously in order to simulate the rolling action. The stresses and deformation results were compared with experimental data. Based on the stresses analysis and experimental tests, it reveals that separating force should be strictly controlled in the twin roll casting process in order to avoid cracks caused by thermal and deformation stresses.

Key words: twin roll casting, visco-plasticity constitutive model, stress and deformation analysis, magnesium alloy.

Copyright © 2009 by IPPT PAN

1. Introduction

TWIN-ROLL CASTING PROCESS is a rapid solidification process combined with hot rolling. In the process, molten metal is solidified starting at the point of first metal-roll contact and ending before the kissing point. This near-net-shape process can directly produce thin strips in one step. It has more advantages due to its higher productivity, low cost and energy saving. Therefore more and more researchers have concentrated their studies on these processes [1–3]. Calculation of stress for twin roll casting process is difficult and complex due to the high temperature gradient for both the melt and solid states in the solidified region with the combination of rolling and bending actions. Therefore, in some simulations the rolling process is usually simplified or even not considered; sometimes only thermal stresses are calculated [4, 5].

There are some important aspects in stresses modeling that must be considered in the casting process [6]. These include the effects of anisotropic properties, phase

transformations, interaction with the mold, fluid flow, temperature dependence of the elastic modulus, properties of liquid material, combined creep and plasticity, microstructure effects, mesh refinement, and two-dimensional stress states etc. However, in the twin roll casting process rolling plays an important role and the liquid metal is squeezed out from the mushy zone, which is very different from the conventional continuous casting process. Therefore, the constitutive equations for cast materials must take into account the wide range of temperature under which the stresses and deformation occur, including the temperature level at the melting point. In order to describe the behavior traditionally called visco-plastic, these models also aim to describe creep, especially at higher temperatures. Recently, a set of internal type constitutive equations for large elastic-viscoplastic deformation at high temperature was proposed by ANAND and BROWN [7–9]. Some research works have used the Anand’s model in numerous application problems [10, 15]. In this work, we focus our research on the constitutive equation, stresses and deformation study, while other aspects are simplified. A 2D FEM model is employed and sequential coupled analysis method is used to simulate the thermo-mechanical behavior during twin-roll casting process of Mg alloy AZ31. Firstly, the thermal fluid flow of twin-roll casting process was simulated by using a CFD model based on ANSYS FLOTRAN; then the Anand’s model, a temperature and rate-dependent model for high temperature deformation, was employed to calculate the thermal mechanical stress in the casting process.

2. Thermal flow simulation

2.1. Theoretical equation and boundary conditions

The schematic drawing of twin-roll casting process is shown in Fig. 1. There were 7161 Nodes and 6900 elements in the 2D FEM model.

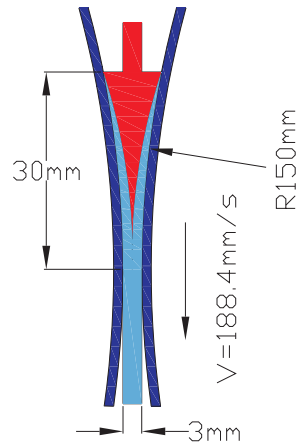


FIG. 1. Schematic drawing of twin-roll casting process.

Considering the symmetry, only half of the twin-roll casting model was employed. The governing Navier-Stokes equation combined with continuity equation, thermal transport equation and constitutive property relationship are given by Eq. (2.1):

$$(2.1) \quad \frac{\partial}{\partial x_k}(\rho C_\Phi V_k \Phi) + \frac{\partial}{\partial t}(\rho C_\Phi \Phi) = \frac{\partial}{\partial x_k} \left(\Gamma_\Phi \frac{\partial \Phi}{\partial x_k} \right) + S_\Phi.$$

Here ρ is the density, Φ represents the dependent variable, and C_Φ , Γ_Φ , and S_Φ indicate transient and diffusion coefficients and the source term, respectively, which are listed in Table 1.

Table 1. Representation of the terms in the transport equations.

Φ	Equations	C_Φ	Γ_Φ	S_Φ
1	Continuity equation	1	0	0
T	Energy equation	c	λ	Q_r
V_i	Momentum equation	1	μ_e	$-\frac{\partial P}{\partial x_k} + \Delta \rho g_k$

Here V_i denote the components of the velocity vector in the x_i directions. In energy equation, T , c , λ and Q_r indicate temperature, specific heat, conductivity coefficient and internal heat source, respectively. P and μ_e indicate pressure and the effective viscosity. g_k denotes the components of acceleration due to gravity and the field force applied to the fluid domain. The time-averaging k - ε model has been used to solve the fluid flow equations.

The casting conditions are as follows: the roll gap was set at 3 mm; roll diameter 300 mm; the casting speed was 188.4 mm/min; casting temperature 958 K; set-back distance 30 mm; strip/roll heat transfer coefficient 15000 W/(m² · K).

2.2. Simulation results of thermal flow

The material parameters of AZ31 are as follows: density 1680 kg/m³; solid temperature 848 K; liquid temperature 903 K; heat conductivity 51 W/(m · K); latent heat 372000 J/(kg · K). The viscosity is temperature-dependent and the equivalent specific heat method was adopted to deal with latent heat. Following assumptions were made for the thermal flow simulation: heat transfer coefficient on the strip/roll interface is constant; rollers surface temperature is 373 K; side dams and nozzle are in adiabatic conditions; non-slip on roll/metal interface.

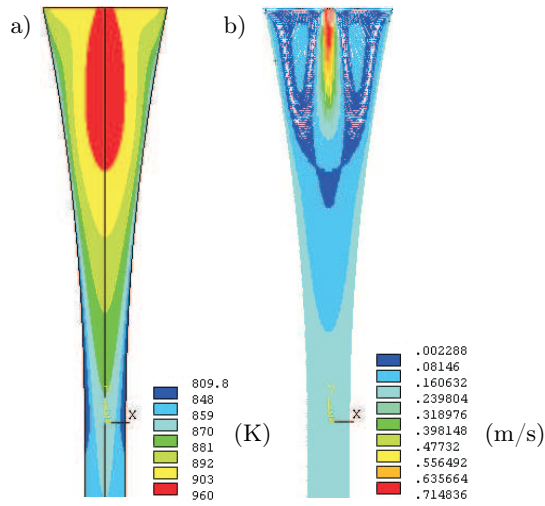


FIG. 2. Thermal flow simulation results: a) temperature field, b) velocity field.

Based on these assumptions, steady-state simulations are performed. Thermal flow simulation results are shown in Fig. 2. These results will be applied as a thermal load in thermal-mechanical stresses.

3. Inelastic constitute equation

3.1. Total strain rate

In the twin-roll thin strip casting process, stresses primarily arise due to high thermal gradient and rolling deformation. The total strain rate can be decomposed as:

$$(3.1) \quad \dot{\varepsilon}_{ij} = \dot{\varepsilon}_{ij}^e + \dot{\varepsilon}_{ij}^p + \dot{\varepsilon}_{ij}^{th},$$

where $\dot{\varepsilon}_{ij}^e$, $\dot{\varepsilon}_{ij}^p$ and $\dot{\varepsilon}_{ij}^{th}$ are elastic, plastic and thermal strain rates, respectively.

Relationship between the elastic strain rate and rate of stress tensor is given by:

$$(3.2) \quad \dot{\sigma}_{ij} = E_{ijkl}(T)\dot{\varepsilon}_{kl}^e,$$

where $E_{ijkl}(T)$ is the temperature-dependent elastic modulus.

Thermal strain rate is given by:

$$(3.3) \quad \dot{\varepsilon}_{ij}^{th} = \alpha \Delta \dot{T} \delta_{ij},$$

where $\Delta \dot{T}$ is the change rate of current temperature and the reference temperature at the point, α is the thermal coefficient of expansion.

The plastic strain rate is described by the Anand model, which is a temperature and rate-dependent model for high temperature in the large deformation process.

3.2. Anand model

A set of internal-type constitutive equations for large elastic-viscoplastic deformation at high temperature was proposed by ANAND and BROWN [7–9]. There are two basic features in this model. First, this model needs no explicit yield condition and no loading/unloading criterion. The plastic strain is assumed to take place at all nonzero stress values, although at low stresses the rate of plastic flow may be immeasurably small. Second, this model employs a single scalar as an internal variable to represent the isotropic resistance to plastic flow offered by the internal state of the material. The internal variable s represents an averaged isotropic resistance to macroscopic plastic flow offered by the underlying isotropic strengthening mechanisms.

The evolution equation for the stress T_{ij} :

$$(3.4) \quad T_{ij}^{\nabla} = E_{ijkl}[D_{kl} - D_{kl}^p]$$

with

$$(3.5) \quad N_{kl} = \sqrt{3/2}(T'_{kl}/\tilde{\sigma}),$$

$$(3.6) \quad D_{kl}^p = \sqrt{3/2}\dot{\tilde{\epsilon}}^p N_{kl},$$

$$(3.7) \quad \tilde{\sigma} = \sqrt{(3/2)T'_{ij}T'_{ij}},$$

where T_{ij}^{∇} is the Jaumann derivative of Cauchy stress T_{ij} , E_{ijkl} is the elasticity modulus, D_{kl} is the stretching tensor. $\tilde{\epsilon}^p$ is the equivalent plastic strain rate, N_{kl} is the direction of plastic flow, T'_{ij} is the deviator of the Cauchy stress, $\tilde{\sigma}$ is the equivalent stress.

The specific functional form for the flow equation:

$$(3.8) \quad \dot{\tilde{\epsilon}}^p = A \exp\left(-\frac{Q}{R\theta}\right) \left[\sinh\left(\xi \frac{\tilde{\sigma}}{s}\right) \right]^{1/m}$$

and the specific functional form of evolution equation for the internal variable s

$$(3.9) \quad \dot{s} = \left\{ h_0 \left| \left(1 - \frac{s}{s^*}\right) \right|^a \operatorname{sign}\left(1 - \frac{s}{s^*}\right) \right\} \dot{\tilde{\epsilon}}^p; \quad a > 1$$

with

$$(3.10) \quad s^* = \tilde{s} \left[\frac{\dot{\tilde{\epsilon}}^p}{A} \exp\left(\frac{Q}{RT}\right) \right]^n,$$

where h_0 is the hardening constant, A is the strain-rate sensitivity of hardening, s^* is the saturation value of s , \tilde{s} is a coefficient, and n is the strain-rate sensitivity for the saturation value of deformation resistance, respectively.

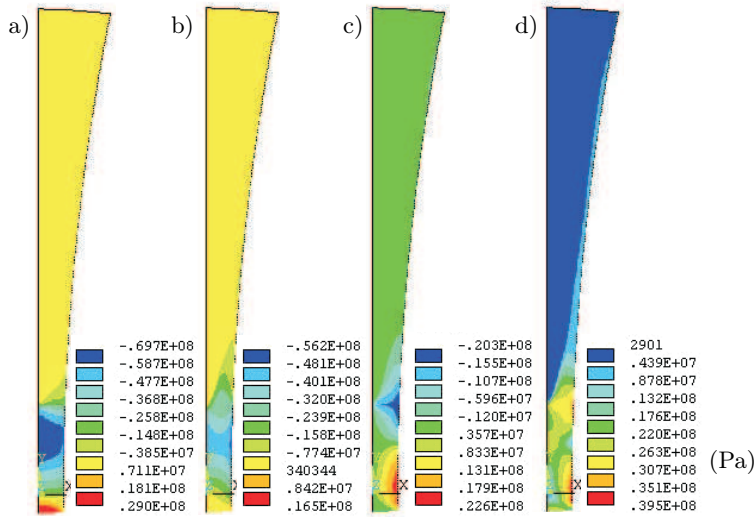


FIG. 3. Contours of σ_x (a), σ_y (b), σ_{xy} (c) and von Mises stress (d).

The nine parameters of Anand constitutive model A , Q , ξ , m , h_0 , n , a and s_0 (the initial value of s) can be obtained from curve-fitting of the compression tests, by which large strain and fully developed plastic flow can be achieved due to the absence of necking. Isothermal constant true strain rate tests of AZ31 with different strain rates and temperatures were carried out, the true strain versus the stress curves were shown in Fig. 3. The parameters of Anand model regressed from comparison tests are A : $3.5 \times 10^7 \text{ s}^{-1}$, Q : 160 kJ/mol, ξ : 8.5, m : 0.28, h_0 : $3.038 \times 10^9 \text{ Pa}$, n : 0.018, a : 1.07, s_0 : $3.5 \times 10^7 \text{ Pa}$, \tilde{s} : $5 \times 10^7 \text{ Pa}$. Figure 4 show the predicted and experimental strain stress-curves.

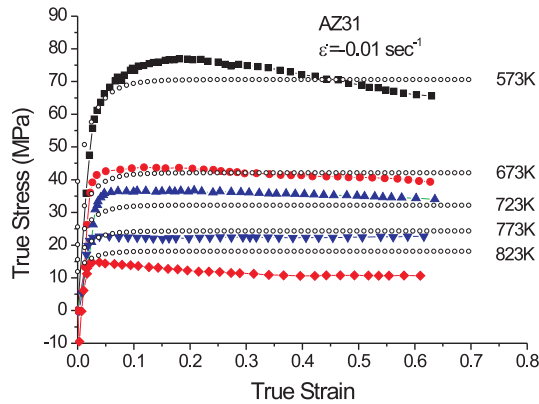


FIG. 4. Prediction and experimental compression of true strain vs. stress curves at different temperatures.

3.3. Thermal Stresses

Since both the liquid and solid regions are parts of the calculation domain, a special procedure is employed to handle the liquid region [4]. A value of Poisson's ratio very close to 0.5 is assigned at the nodes where temperature is above the coherence temperature. This makes the liquid phase close to being incompressible under mechanical loading. The Young's modulus is set to a very small number at the nodes above the coherence temperature.

In this study, ANSYS structural model was employed to calculate the stresses. The thermal flow result was assumed as body load and the reference temperature was assumed as the average temperature of the strip surface [5]. The strip surface set as free surface because solidifying shrinkage.

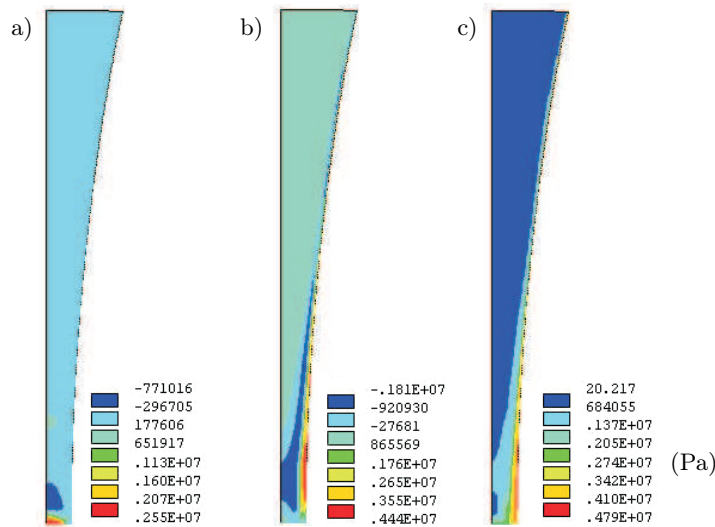


FIG. 5. Contours of σ_x (a), σ_y (b) and von Mises stress (c).

The results of calculations of thermal stresses are shown in Fig. 5. The states of stress at the strip surface along the casting direction is tensile; this is one of the main reasons causing strip crack defects. From these results, it can be seen that the stress level near to the roll gap has suddenly grown due to changes of visco-plastic strain in the strip near the roll gap. The change of thickness in the roll gap is mainly according to the influence of the viscous deformation and the heat expansion deformation.

3.4. Thermal mechanical stresses

Displacement load along the roller tangent direction is imposed to simulate rolling in the twin-roll casting process. The results of calculations and deformations are shown in Fig. 6 and Fig. 7, respectively.

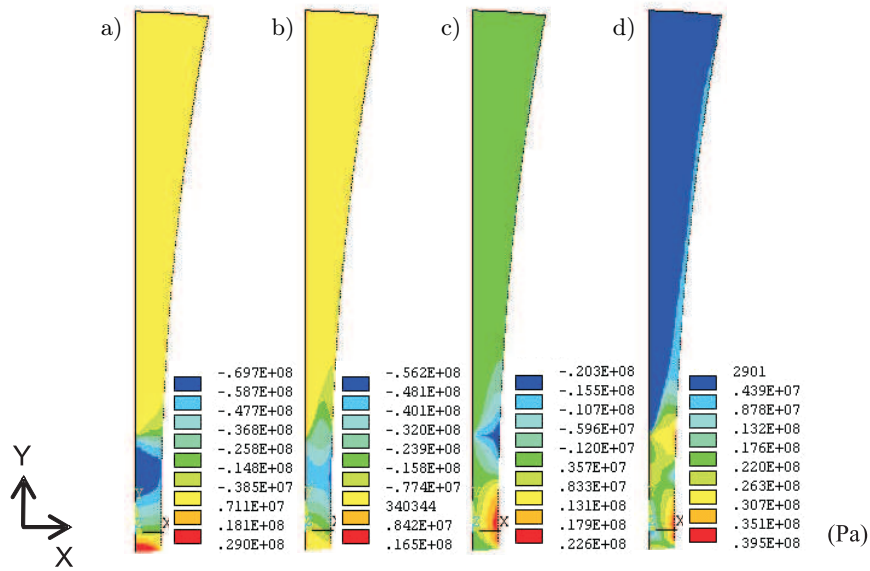


FIG. 6. Contours of σ_x (a), σ_y (b), σ_{xy} (c) and von Mises stress (d).

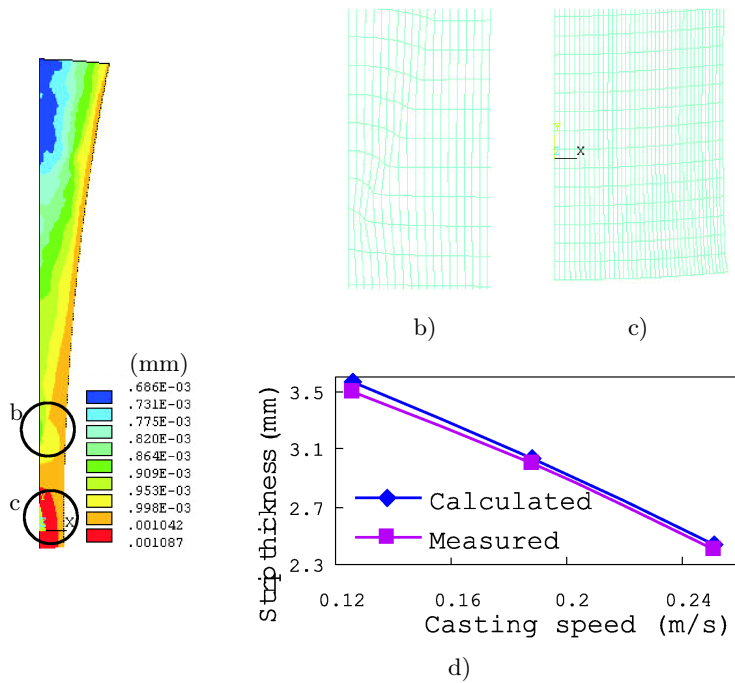


FIG. 7. Contour of deformation (a), the enlarged details of mesh deformation near the coalescent zone (b) and exit zone (c), denoted in (a). Comparison of strip thickness between the measured and calculated data at different casting speed and the same separating force (d).

4. Discussion

In the twin-roll casting, the process is very similar to a hot rolling process. Neutral point, forward slip and backward slip exist if the solidification end point is located before the kissing point. Figure 7b shows that when the two pieces of solidified shells come together, severe deformation occurs in the coherence region and the liquid metal in the mushy zone will be crushed out. From these results, we can know that the change of thickness in the roll gap depends on the influence of the viscous deformation and the heat expansion deformation. The continuous casting process is the reason that the grains morphology at the central region of the strip is very different from that at the surface. The rolling action has increased with the increase of the casting speed. Figure 8 shows the effect of casting speed on the grain morphology.

Good quality of the results follows from the fact that the cast strip was obtained by strict control of the separating force. Figure 7d shows the comparison of the measured and calculated strip thickness at different casting speed and the same separating force.

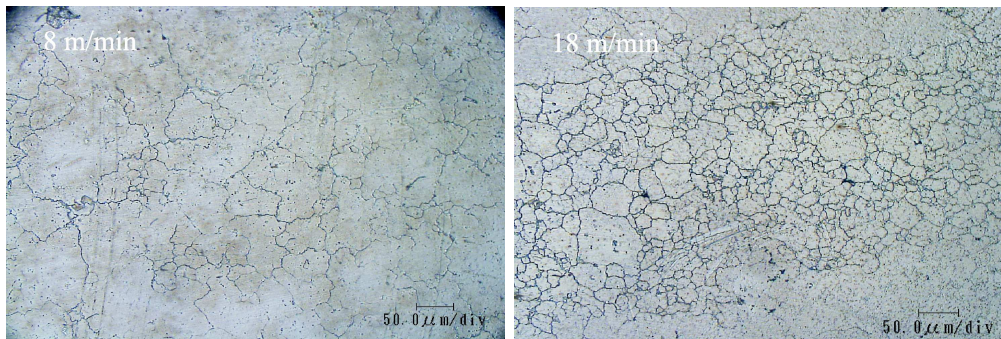


FIG. 8. Refined grains in the central part of the strip due to the effect of casting speed.

Non-uniform deformation along the thickness of is due to the high temperature gradient; this non-uniform deformation leads to the increase of the tendency to crack defects of the strip surface. Figure 6c shows that there are two high shear stress regions: one is located near the coherence point caused by backward slip and the other one occurs near the exit point caused by forward slip. Figure 6d shows the same tendency. In the twin roll casting process, the curved and solidified shells will come together and become straight. This bending action will also increase the stress level near the coherence region.

5. Conclusion

The deformation of twin-roll casting process is non-uniformed because of high temperature gradient; the backward squeeze zone and the exit zone are the two dangerous regions for cracks. Rolling actions is much more dangerous than the thermal stress. Control of the solidification end near the kissing point can cause the decrease of the rolling deformation and decrease of the crack tendency.

On the basis of the stresses analysis and experimental tests, it follows that separating force should be strictly controlled in the twin roll casting process in order to avoid the cracks caused by thermal and deformation stresses.

Acknowledgments

The support provided by High Technology Research Center (HRC) and Open Research Center (ORC) in the Saitama Institute of Technology for this work is gratefully acknowledged.

References

1. D.Y. JU, H.Y. ZHAO, X.D. HU, *Thermal Flow Simulation on Twin Roll Casting Process for Thin Strip Production of Magnesium Alloy*, Mater. Sci. Forum, **488–489**, 439, 2005.
2. O. DAALAND, A.B. ESPEDAL, M.L. NEDREBERG, I. ALVESTAD, *Thin Gauge Twin-roll Casting Process Capabilities and Product Quality*, Light Metals, 745, 1997.
3. R.I.L. GUTHRIE, R.P. TAVARES, *Mathematical and Physical Modeling of Steel Flow and Solidification in Twin-roll/Horizontal Belt Thin-strip Casting Machines*, Applied Mathematics Modelling, **22**, 851, 1998.
4. M. GUPTA, Y. SAHAI, *Mathematical Modeling of Thermally Induced Stresses in Two-roll Melt Drag Thin Strip Casting of Steel*, ISIJ International, **40**, No. 2, 144–152, 2000.
5. Y. SAHAI, A. SAXENA, *Modeling of Twin-roll Thin Strip Casting of Aluminum Alloys*, Light Metals, TMS, 643–650, 2002.
6. B.G. THOMAS, *Issues in Thermal-mechanical Modeling of Casting Processes*, ISIJ International, **35**, No. 6, 737–743, 1995.
7. S.B. BROWN, K.H. KIM, L. ANAND, *An Internal Variable Constitutive Model for Hot Working of Metals*, International Journal of Plasticity, **5**, 95–130, 1989.
8. A.M. LUSH, G. WEBER, L. ANAND, *An implicit time-integration procedure for a set of internal variable constitutive equations for isotropic elasto-viscoplasticity*, International Journal of Plasticity, **5**, 521–549, 1989.
9. G.G. WEBER, A.M. LUSH, A. ZAVALIANGOS, L. ANAND, *An objective time-integration procedure for isotropic rate-independent and rate-dependent elastic-plastic constitutive equations*, International Journal of Plasticity, **6**, 701–744, 1990.
10. C. XU, G. CHEN, M. SAKANE, *Modified Anand Constitutive Model for Lead-free Solder Sn-3.5Ag*, Inter. Society Conference on Thermal Phenomena, 447–452, 2004.

11. J. KOIKE, *Dislocation Plasticity and Complementary Deformation Mechanisms in Polycrystalline Mg Alloys*, Materials Science Forum, **449–452**, 665–669, 2004.
12. K. MINAMI *et al.*, *Mathematical Modeling of Mean Flow Stress during the Hot Strip Rolling of Nb Steels*, ISIJ International, **36**, 1507–1515, 1996.
13. G.F. QUAN, *Yield and Plastic Deformation of Mg-Alloy AZ31 at Elevated Temperatures*, Materials Science Forum **488–489**, 623–628, 2005.
14. B.H. LEE *et al.*, *High Temperature Deformation Behavior of Strip-Cast AZ31 Mg Alloy*, Advanced Materials Research, **15–17**, 461–466, 2007.
15. M. NODAL *et al.*, *Biaxial Tensile Deformation Behavior and Microstructural Evolutions of Superplasticity in AZ31 Magnesium Alloy*, Materials Science Forum, **551–552**, 225–230, 2007.

Received October 22, 2008; revised version July 7, 2009.
